

DES SIMULATION OF THE FLOW AROUND A CIRCULAR CYLINDER IN GROUND EFFECT

Luciano Gonçalves Noletto, lucianoletto@unb.br

Antonio C. P. Brasil Junior, brasiljr@unb.br

Universidade de Brasília, Faculdade de Tecnologia, Departamento de Engenharia Mecânica, Laboratório de Energia e Ambiente, 70910-900 - Asa Norte - Brasília, DF - Brasil

Jhon Nero Vaz Goulart, jvaz@unb.br

Manuel Nascimento Dias Barcelos Júnior, manuelbarcelos@gmail.com

Universidade de Brasília, Faculdade UnB Gama, Área Especial 2 Lote 14 Setor Central Gama-DF

Abstract. *Two-dimensional detached eddy simulations were conducted on the turbulent flow over a circular cylinder close to a ground wall. This type of flow receives heavy interference from the boundary layer developed by the wall. The ground effect can be identified by the presence of a recirculation zone at the wall, which moves downstream as the time passes. Although there are several researches concerning the flow over cylinders close to walls, many obscure points exists. The present work uses a hybrid turbulence modeling, discretized by a finite element incremental projection scheme, which is based in a methodology of pressure correction. The present work uses the following implementation: The pressure is maintained at the first substep and corrected at the next substep to be used to project the velocity at the final substep. The results showed the generation and development of vortex shedding. The aero dynamical coefficients show the oscillatory pattern of the flow. The obtained results are similar with other results at the literature.*

Keywords: *Ground Effect, Vortex shedding, Detached Eddy Simulation*

1. INTRODUCTION

The complete understanding of the flow around bluff bodies is an aim for several researches. It has an engineering interest in several engineering areas, such as flow induced vibration, hydrodynamical loads in planes and ships for instance. Complete solutions of the boundary layer behavior are necessary because it can answer questions about the separation point, the transition to turbulence and how the viscous wake is influenced by the surface of the cylinder (Bimbatto et al., 2009). Generated vorticity close to the cylinder surface is projected to the viscous flow, which develop and produces harmonic loads in solid structures, which synchronized with vortex shedding, can affect its structural integrity.

Experimental studies of the flow over cylinders close to a ground are conducted by Zdravkovich (1985), Bearman and Zdravkovich (1978), and Lei et al. (1999), amongst others. The authors stated that the characteristics of the dynamical loads are not only dependant of the Reynolds number, but also to the non-dimensional parameter h/d . On this parameter, h is the height between the ground and the center of the cylinder and d is the diameter of the cylinder. The relation height-diameter is appointed as the main non-dimensional parameter for this kind of flow. Studies of the vortex shedding characteristics at the wake of a cylinder close to a ground plane were conducted by Nishino et al. (2008). The simulated Reynolds number were put as 10^4 and 10^5 . Four values of h/d were simulated. The authors found three fundamental vortex shedding regimes: large-gap regimes ($h/d > 0,50$), intermediate gap regimes ($0,35 < h/d < 0,50$) and small gap regimes ($h/d < 0,35$). The numerical simulation showed that the Von Kármán vortex shedding occurred at the immediate downstream of the cylinder for large gaps. For other regimes, the shedding were halted, producing wakes with little vortex formations.

The present study will show results of the simulation of the flow over a cylinder close to a plane for a h/d value of 0,50. Detached eddy simulation based on the SST turbulence model will be employed in a finite element method context. A projection method will be used as the numerical algorithm. This paper will show flow visualization and instantaneous values of the drag and lift coefficient. Those results will be compared with the results of Nishino et al. (2008)

2. Problem Statement

The mass conservation and momentum equations for incompressible flows are written in a framework of turbulence modeling and defined in an open connected bounded domain $\Omega_t \times [0, T]$ in \mathbb{R}^d (where $d=2$ or 3) with boundary $\Gamma_t = \partial\Omega_t$ such as:

$$\nabla \cdot \mathbf{u} = 0 \quad (1)$$

$$\frac{\partial \mathbf{u}}{\partial t} + \mathbf{u} \cdot \nabla \mathbf{u} = -\frac{1}{\rho} \nabla p + (\nu + \nu_T) \nabla^2 \mathbf{u} + f \quad (2)$$

In those equations \mathbf{u} and p are the mean velocity and pressure fields, ν and ν_T are the kinematic and turbulent viscosity, respectively, ρ is the fluid density and f is the source term. One can note that the problem is open, since the turbulent

viscosity needs modeling. The modeling approach is given by the SST turbulence model (Menter et al.,2003):

$$\frac{\partial k}{\partial t} + \mathbf{u} \cdot \nabla k = P_k - \beta' k \omega + \nabla \cdot \left[\left(\nu + \frac{\nu_t}{\sigma_k} \right) \nabla k \right] \quad (3)$$

$$\begin{aligned} \frac{\partial \omega}{\partial t} + \mathbf{u} \cdot \nabla \omega &= \alpha S^2 + \beta \omega + \nabla \cdot \left[\left(\nu + \frac{\nu_t}{\sigma_\omega} \right) \nabla \omega \right] \\ &+ 2(1 - F_1) \sigma_{\omega 2} + \frac{1}{\omega} (\nabla k) (\nabla \omega) \end{aligned} \quad (4)$$

Here, k and ω are the turbulent kinetic energy and turbulent frequency respectively. The eddy viscosity is defined by:

$$\nu_t = \frac{\alpha_1 k}{\max(\alpha_1 \omega, S F_2)} \quad (5)$$

S is an invariant measure of the rate-of-strain tensor and the blending functions F_1 and F_2 are given as follows:

$$F_1 = \tanh(\arg_1^4) \quad (6)$$

$$\arg_1 = \min \left[\max \left(\frac{\sqrt{k}}{\beta' \omega y}, \frac{500 \nu}{y^2 \omega} \right), \frac{4k}{C D_{k\omega} \sigma_{\omega 2} y^2} \right] \quad (7)$$

$$C D_{k\omega} = \max \left(2 \frac{1}{\omega \sigma_{\omega 2}} \nabla k \nabla \omega, 1, 0 \times 10^{-10} \right) \quad (8)$$

$$F_2 = \tanh(\arg_2^2) \quad (9)$$

$$\arg_2 = \max \left(\frac{2\sqrt{k}}{\beta' \omega y}, \frac{500 \nu}{y^2 \omega} \right) \quad (10)$$

Here, y is the distance to the nearest wall. A production limiter is used to avoid the excessive generation of turbulence in stagnation points:

$$P_k = \mu_t S^2 \quad (11)$$

$$\widetilde{P}_k = \min(P_k, 10 \cdot \rho \beta^* k \omega) \quad (12)$$

The constants of the model are accounted as a linear combination of the corresponding constants of the $k - \varepsilon$ and $k - \omega$ models:

$$\alpha = \alpha_1 F_1 + \alpha_2 (1 - F_1) + \dots \quad (13)$$

The constants are $\beta = 0.09$, $\alpha_1 = 5/9$, $\beta_1 = 3/40$, $\alpha_{k1} = 0.5$, $\sigma_{\omega 1} = 0.5$, $\alpha_2 = 0.44$, $\beta_2 = 0.0828$, $\sigma_{k2} = 1$, $\sigma_{\omega 2} = 0.856$. The ω -equation allows a near-wall formulation, which gradually switches from wall-functions to low-Reynolds near wall formulations (Menter et al.,2003).

The DES SST formulation uses the SST turbulence model formulation with a modification of the k -equation destruction term (Strelets (2001)):

$$k \beta' \omega \Rightarrow k \beta' \omega F_{DES} \quad (14)$$

The DES blending function is given as follows:

$$F_{DES} = \max \left(\frac{\sqrt{k}}{C_{DES} \Delta \beta' \omega}, 1 \right) \quad (15)$$

Here, Δ is the maximum local grid spacing and $C_{DES} = 0,61$ is a calibration constant. The boundary conditions are given by:

$$\mathbf{u}(x, t) = \mathbf{u}_d; \quad \text{on } \Gamma_d \quad (16)$$

$$p(x, t) = p_{\text{ref}}; \quad \text{on } \Gamma_o \quad (17)$$

$$k(x, t) = k_d; \quad \text{on } \Gamma_d \quad (18)$$

$$\omega(x, t) = \omega_d; \quad \text{on } \Gamma_d \quad (19)$$

For the above mentioned conditions, Γ_d represents the boundary where Dirichlet-type boundary conditions (\mathbf{u}_d , k_d , ω_d) are prescribed. Γ_o denotes the boundary where a reference pressure p_{ref} is prescribed.

3. Numerical Methodology

The following methodology is designed to solve the equation system (1)-(4) by a semi-explicit iterative strategy, after time and spatial discretization. A framework of projection methods, given by Donea and Huerta (2003), Goldberg and Ruas (1999) and Lohner et al. (2006). is employed. One can define a time step $\Delta t > 0$ where a set of variables denoted by $(\mathbf{u}^n, p^n, k^n, \omega^n)$ is defined. The set of variables $(\mathbf{u}^{n+1}, p^{n+1}, k^{n+1}, \omega^{n+1})$ at the time $t + \Delta t$, is obtained by velocity and pressure splitting and calculation of turbulent quantities, given as follows:

$$\frac{1}{\Delta t} (\mathbf{u}^* - \mathbf{u}^n) + \mathbf{u}^n \cdot \nabla \mathbf{u}^n = -\frac{1}{\rho} \nabla p^n + (\nu + \nu_T) \nabla^2 \mathbf{u}^n + f \quad (20)$$

$$\frac{1}{\Delta t} (\mathbf{u}^{n+1} - \mathbf{u}^*) = -\frac{1}{\rho} \nabla (p^{n+1} - p^n) \quad (21)$$

$$\nabla \cdot \mathbf{u}^{n+1} = 0 \quad (22)$$

$$\frac{1}{\Delta t} (k^* - k^n) + \mathbf{u}^n \cdot \nabla k^n = \left(\nu + \frac{\nu_t}{\sigma_k} \right) \nabla^2 k^n + f_k \quad (23)$$

$$\frac{1}{\Delta t} (\omega^* - \omega^n) + \mathbf{u}^n \cdot \nabla \omega^n = \left(\nu + \frac{\nu_t}{\sigma_\omega} \right) (\nabla^2 \omega^n) + f_\omega \quad (24)$$

Where:

$$f_k = P_k - \beta' k \omega \quad (25)$$

$$f_\omega = \alpha S^2 + \beta \omega^n + 2(1 - F_1) \sigma_{\omega^2} + \frac{1}{\omega^n} (\nabla k) (\nabla \omega^n) \quad (26)$$

This algorithm introduces predicted quantities \mathbf{u}^* , k^* and ω^* . From those, only \mathbf{u}^* will be corrected at each step. This algorithm transforms one problem into a sum of two problems: One made by a pure advection and other made by pure diffusion. Both are solved sequentially at each step of the time integration (Donea and Huerta (2003)). When one takes the divergent of equation 21 and uses on equation 22, the pressure equation assumes the form of a Poisson equation:

$$\nabla^2 (p^{n+1} - p^n) = \frac{\rho}{\Delta t} \nabla \cdot \mathbf{u}^* \quad (27)$$

The boundary condition for this equation is given as follows:

$$\nabla (p^{n+1} - p^n) \cdot \mathbf{n} = \frac{\rho}{\Delta t} \mathbf{u}^* \cdot \mathbf{n} \text{ on } \Gamma_o \quad (28)$$

Remark:

The described projection algorithm is called Incremental Projection Scheme (Minev, 2001, Zhang, 2007). It is based on a pressure correction methodology. These schemes are time-marching techniques composed of substeps at each time step. The pressure can be treated explicitly or ignored at the first substep. Its solution will be used to project the velocity into a divergent-null field. The present work uses the following implementation: The pressure is maintained at the first substep and corrected at the next substep to be used to correct the velocity at the final substep. This implementation improves convergence properties, as reported at the literature (Guermont et al., 2006, Codina, 2001).

3.1 Standard Weak Form

Some definitions must be presented in order to show the standard weak form. One can denote $L^2(\Omega_t)$ as the space of squared integrable functions over the domain Ω_t and $H^1(\Omega_t)$ as the Sobolev space where its derivatives are also squared integrable. The internal product of $L^2(\Omega_t)$ is denoted by $(\cdot, \cdot) = \int_{\Omega_t} \cdot \cdot d\Omega_t$ and $H_0^1(\Omega_t)$ is the sub-space of functions with zero value on boundaries.

One can write weight functions $\mathbf{v} \in V = H_0^1(\Omega_t)$ and $q \in Q = L^2(\Omega_t)/\mathbb{R}$, and consider $\mathbf{u} \in U = H^1(\Omega_t)$. The weak form of equations 20, 21, 23, 24 and 27 can be written as follows:

$$m_u(\Delta \mathbf{u}^*, \mathbf{v}) + c_u(\mathbf{u}^n, \mathbf{u}^n, \mathbf{v}) + (\nu + \nu_T) a_u(\mathbf{u}^n, \mathbf{v}) + \frac{1}{\rho} b(p, \mathbf{v}) = (f, \mathbf{v}) \quad (29)$$

$$a(\Delta p, q) = -\frac{\rho}{\Delta t} b(\mathbf{u}^*, q) \quad (30)$$

$$m(\Delta \mathbf{u}^{n+1}, \mathbf{v}) = -\frac{1}{\rho} b(\Delta p, \mathbf{v}) \quad (31)$$

$$m_k(\Delta k^*, \mathbf{v}) + c_k(k^n, \mathbf{u}^n, \mathbf{v}) + D_k a_k(k^n, \mathbf{v}) = (f_k, \mathbf{v}) \quad (32)$$

$$m_\omega(\Delta \omega^*, \mathbf{v}) + c_\omega(\omega^n, \mathbf{u}^n, \mathbf{v}) + D_\omega a_\omega(\omega^n, \mathbf{v}) = (f_\omega, \mathbf{v}) \quad (33)$$

Where:

$$D_k = \left(\nu + \frac{\nu_T}{\sigma_k} \right) \quad (34)$$

$$D_\omega = \left(\nu + \frac{\nu_T}{\sigma_\omega} \right) \quad (35)$$

Where the following forms are introduced:

$$m_u(\mathbf{u}, \mathbf{v}) := \frac{1}{\Delta t} (\mathbf{u}, \mathbf{v}); \quad c_u(\mathbf{u}, \mathbf{u}, \mathbf{v}) := (\mathbf{u} \cdot \nabla \mathbf{u}, \mathbf{v}) \quad (36)$$

$$a(\mathbf{u}, \mathbf{v}) := (\nabla \mathbf{u}, \nabla \mathbf{v}); \quad b(q, \mathbf{v}) := (q, \nabla \cdot \mathbf{v}) \quad (37)$$

$$m_k(k, \mathbf{v}) := \frac{1}{\Delta t} (k, \mathbf{v}); \quad c_k(k, \mathbf{u}, \mathbf{v}) := (\mathbf{u} \cdot \nabla k, \mathbf{v}) \quad (38)$$

$$m_\omega(\omega, \mathbf{v}) := \frac{1}{\Delta t} (\omega, \mathbf{v}); \quad c_\omega(\omega, \mathbf{u}, \mathbf{v}) := (\mathbf{u} \cdot \nabla \omega, \mathbf{v}) \quad (39)$$

The increments of all calculated fields are denoted by:

$$\begin{aligned} \Delta \mathbf{u}^* &= \mathbf{u}^* - \mathbf{u}^n \\ \Delta \mathbf{u}^{n+1} &= \mathbf{u}^{n+1} - \mathbf{u}^* \\ \Delta p &= p^{n+1} - p^n \\ \Delta k^* &= k^* - k^n \\ \Delta \omega^* &= \omega^* - \omega^n \end{aligned} \quad (40)$$

Remark:

The incremental projection method described here is based on a first-order time discretization. Superior order discretizations can be used accordingly with the problem and with desired precision and computational cost. Therefore, the solution of equations 29 to 33 will lead to a consistent formulation of all calculated fields at time $t + \Delta t$.

3.2 Spatial Discretization

Let $T^h(\Omega_t)$ a regular partition of the domain Ω_t where the finite element spaces $Q_h \subset Q$, $V_h \subset V$ and $U_h \subset U$ are constructed. The discrete problem equivalent to the weak form can be written as: Given $u_h^n, p_h^n, k_h^n, \omega_h^n$, find $u_h^{n+1}, p_h^{n+1}, k_h^{n+1}, \omega_h^{n+1} \in U_h \times Q_h$, such as $\forall \{\mathbf{v}_h, q_h\} \in V_h \times Q_h$:

$$\begin{aligned} m_u(\Delta \mathbf{u}_h^*, \mathbf{v}_h) &= -c_u(\mathbf{u}_h^n, \mathbf{u}_h^n, \mathbf{v}_h) - \nu a_u(\mathbf{u}_h^n, \mathbf{v}_h) - \\ &\quad - \frac{1}{\rho} b(p_h, \mathbf{v}_h) - \mathbf{s}_u(\mathbf{u}_h^n, \mathbf{u}_h^n, \mathbf{v}_h) + (f, \mathbf{v}_h) \end{aligned} \quad (41)$$

$$a(\Delta p_h, q_h) = -\frac{\rho}{\Delta t} b(\mathbf{u}_h^*, q_h) \quad (42)$$

$$m(\mathbf{u}_h^{n+1}, \mathbf{v}_h) = -\frac{1}{\rho} b(\Delta p_h, \mathbf{v}_h) \quad (43)$$

$$m_k(\Delta k_h^*, \mathbf{v}_h) + c_k(k_h^n, \mathbf{u}_h^n, \mathbf{v}_h) + D_k a_k(u_h^n, \mathbf{v}_h) = (f_k, \mathbf{v}_h) \quad (44)$$

$$m_\omega(\Delta \omega_h^*, \mathbf{v}_h) + c_\omega(\omega_h^n, \mathbf{u}_h^n, \mathbf{v}_h) + D_\omega a_\omega(\omega_h^n, \mathbf{v}_h) = (f_\omega, \mathbf{v}_h) \quad (45)$$

The extra term at equation 41 ($\mathbf{s}_u(\mathbf{u}_h^n, \mathbf{u}_h^n, \mathbf{v}_h)$) is responsible to ensure stability in convective-dominated regimes. It is written as:

$$\mathbf{s}_u(\mathbf{u}_h^n, \mathbf{u}_h^n, \mathbf{v}_h) = (\mathbf{u}_h^n \cdot \nabla \mathbf{u}_h^n, \Delta t (\mathbf{u}_h^n \cdot \nabla \mathbf{v})) \quad (46)$$

Considering the dimension of the spaces given by $\dim(V_h) = \dim(U_h) = \dim(Q_h) = N$ and base functions denoted by $\{\mathbf{N}_i; i = 1, N\}$ and $\{\mathbf{N}_j; j = 1, N\}$, the discrete problem matrix form is given as follows:

Step 1: Velocity Calculation:

$$\mathbf{M}_u \cdot \Delta \mathbf{u}_h^* = \mathbf{F}_u^*(\mathbf{u}_h^n, \mathbf{v}_h^n, p_h^n) \quad (47)$$

Step 2: Pressure Calculation - Poisson problem:

$$\mathbf{A} \cdot \Delta p_h = \mathbf{F}_p(\mathbf{u}_h^*) \quad (48)$$

Step 3: Velocity projection in a divergent-free space:

$$\mathbf{M}_u \cdot \Delta \mathbf{u}_h^{n+1} = \mathbf{F}_u(\Delta p_h) \quad (49)$$

Step 4: Kinetic turbulent energy calculation:

$$\mathbf{M}_k \cdot \Delta k_h^* = \mathbf{F}_k^*(k_h^n, \mathbf{v}_h^n) \quad (50)$$

Step 5: Turbulent frequency calculation:

$$\mathbf{M}_\omega \cdot \Delta \omega_h^* = \mathbf{F}_\omega^*(\omega_h^n, \mathbf{v}_h^n) \quad (51)$$

Where the matrices \mathbf{M}_u , \mathbf{M}_k and \mathbf{M}_ω are the mass matrices for the velocity and turbulent quantities respectively and \mathbf{A} is the Laplacian matrix for the pressure. Those matrices are given as follows:

$$\mathbf{M}_{ij} = \frac{1}{\Delta t} (\mathbf{N}_i, \mathbf{N}_j) ; \quad \mathbf{A}_{i,j} = (\nabla \mathbf{N}_i, \nabla \mathbf{N}_j) \quad (52)$$

The vectors \mathbf{F}_u^* , \mathbf{F}_p and \mathbf{F}_u are related to the right hand side discretization of the matrix equations on steps 1 to 3. The boundary integral terms, related to the boundary conditions, are added into these vectors.

Remarks:

- The linear system solution of steps 1 and 3 involve the mass matrix. In order to enhance the convergence rate, this matrix is lumped in a diagonal form. The lumping is performed once in the beginning of the iterative process.
- The linear system for the pressure correction problem, step 2, is solved by the Conjugated Gradient Method, preconditioned by the partial Cholesky factorization. This matrix is stored by a Morse strategy, and the preconditioning is also performed once when this matrix is firstly computed.
- The time step is controlled by a weighted average between convective (Δt_{cov}) and diffusive (Δt_{diff}) time steps, given as follows:

$$\Delta t \leq \frac{\Delta t_{cov} \Delta t_{diff}}{\Delta t_{cov} + \Delta t_{diff}} \quad (53)$$

4. RESULTS AND ANALYSIS

The present paper simulated the two-dimensional case of $h/d = 0.5$ displayed on Nishino et al. (2008):

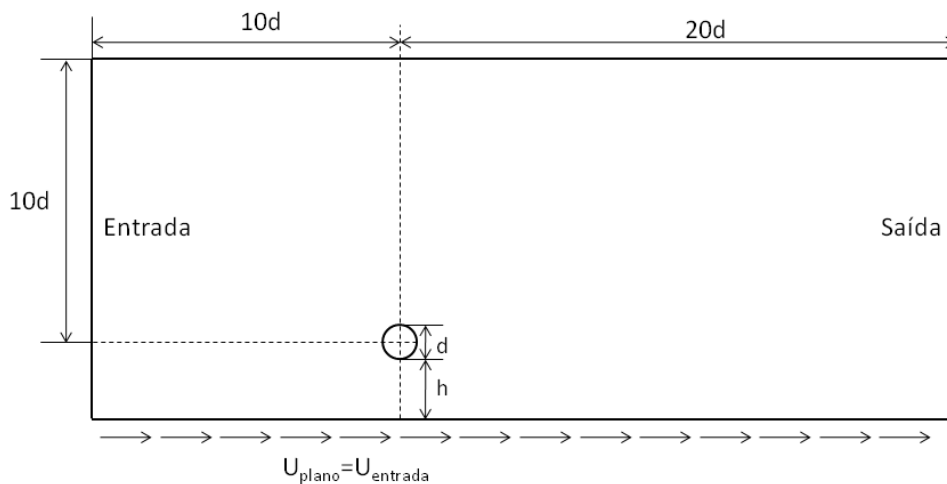


Figure 1. Simulation Domain

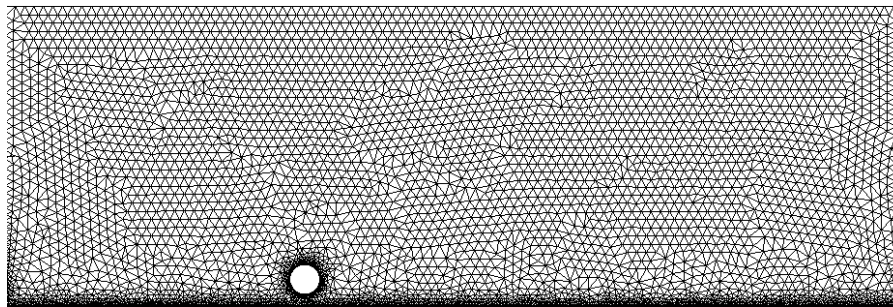


Figure 2. Used Mesh

For the inlet, the velocity was set to give a Reynolds number of 4×10^4 . A zero reference pressure was imposed at the outlet boundary condition. At the cylinder nodes, a no-slip condition was imposed. It was imposed at the plane nodes the inlet velocity to recover the moving ground condition. The used grid has 15992 nodes e 28072 P1 elements. The drag and lift coefficients are given as follows:

$$C_l = \frac{F_l}{0.5\rho U_0^2 A} \quad (54)$$

$$C_d = \frac{F_d}{0.5\rho U_0^2 A} \quad (55)$$

Figures 3 to 6 show the instantaneous flow visualizations. One can note the fast formation of low pressure zones at the cylinder surface. Those zones are converted into vortices that detach from the cylinder, presenting a wake topology close to the classic Von Kármán wake. It is noted that the vortices show a "mushroom" pattern, as seen on Bimbato et al. (2009). Close to the ground, a vorticity region can be seen with symmetrical values of the vortices above, which are shed from the cylinder. This vorticity originates itself at the lower part of the cylinder. Part of the turbulent structures shed from the cylinder adheres to the ground and the other part is transported downstream of the flow. One can note that the ground vorticity moves simultaneously as the shed vortices.

Figure 7 shows the temporal evolution of the aerodynamical coefficients. One can note that the lift coefficients present similar oscillatory behavior. This behavior is related to the vortex shedding, since its frequency has proximity to the Strouhal number for this case. The calculated Strouhal is of 0.2186. Therefore, it can be stated that the vortex shedding has an oscillatory pattern. The drag coefficient showed an oscillatory pattern, but one can note different amplitudes at certain moments. This different amplitudes are explained by the vortices shed and direct themselves to the ground. The average drag coefficient is 1.5167. The delay of boundary layer separation with the variation of the h/d relation is an aim of analysis by Nishino et al. (2007) e Nishino et al. (2008). This delay is an indication of ground effect that affects vortex shedding and formation.

Formation of Von Kármán Vortex Street in two-dimensional bluff bodies is related with the formation of instabilities at the near wake. These instabilities propagate and transition the flow towards the turbulence, generating the vortex shedding (Nishino and Roberts, 2008). The activation of the DES filter that separates large and small scales has a close relationship

with that formation. So, a modification of this filter can anticipate the formation or delay it. The modification can be made in a same way as altering the Smagorinsky constant in Large-eddy simulations. Future work must be made to confirm that assertive. It is important to stress that there are few experimental data about this flow. Therefore, the present simulation was compared with the numerical data obtained by Nishino et al. (2008). The results show resemblance with the results obtained by the reference.

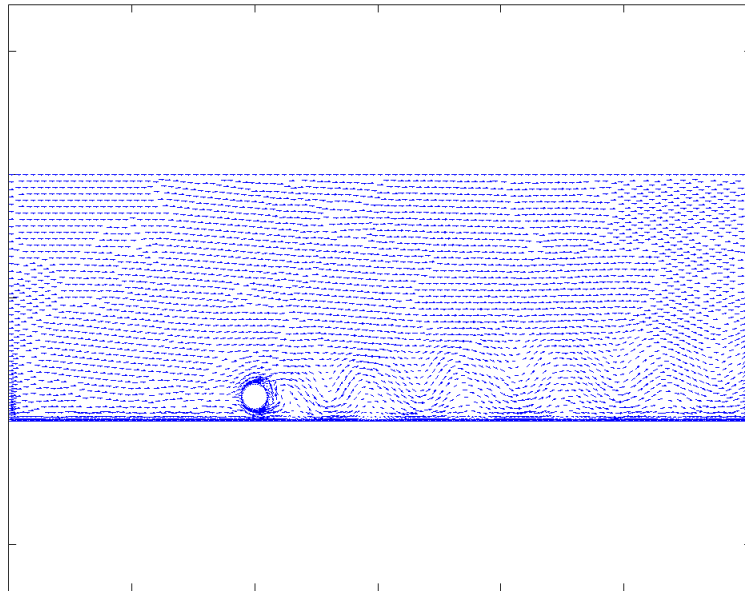


Figure 3. Velocity Vectors

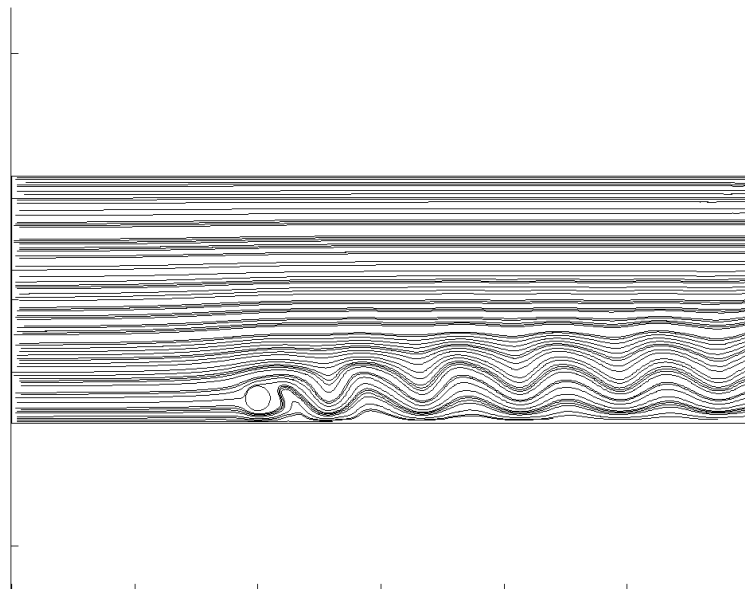


Figure 4. Streamlines

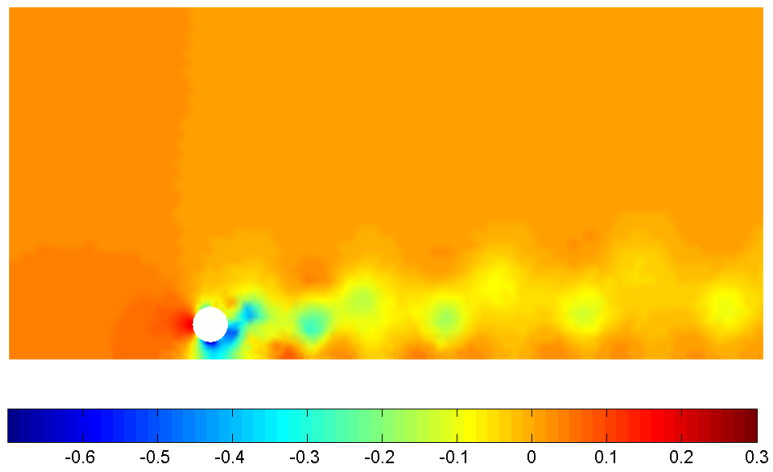


Figure 5. Pressure Contours

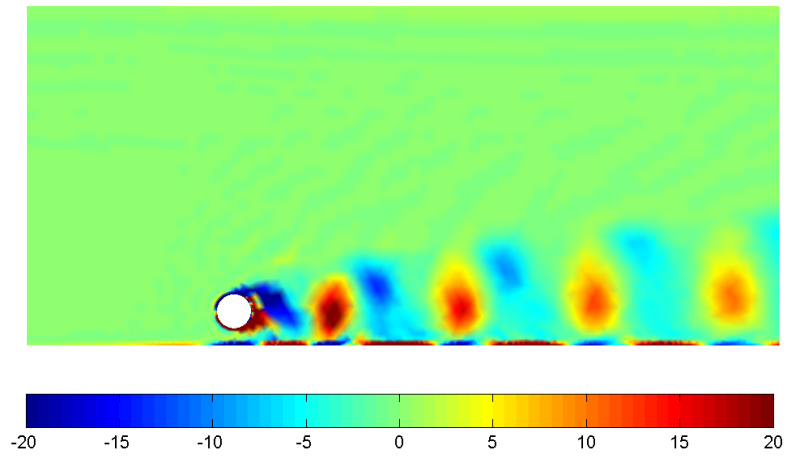


Figure 6. Vorticity

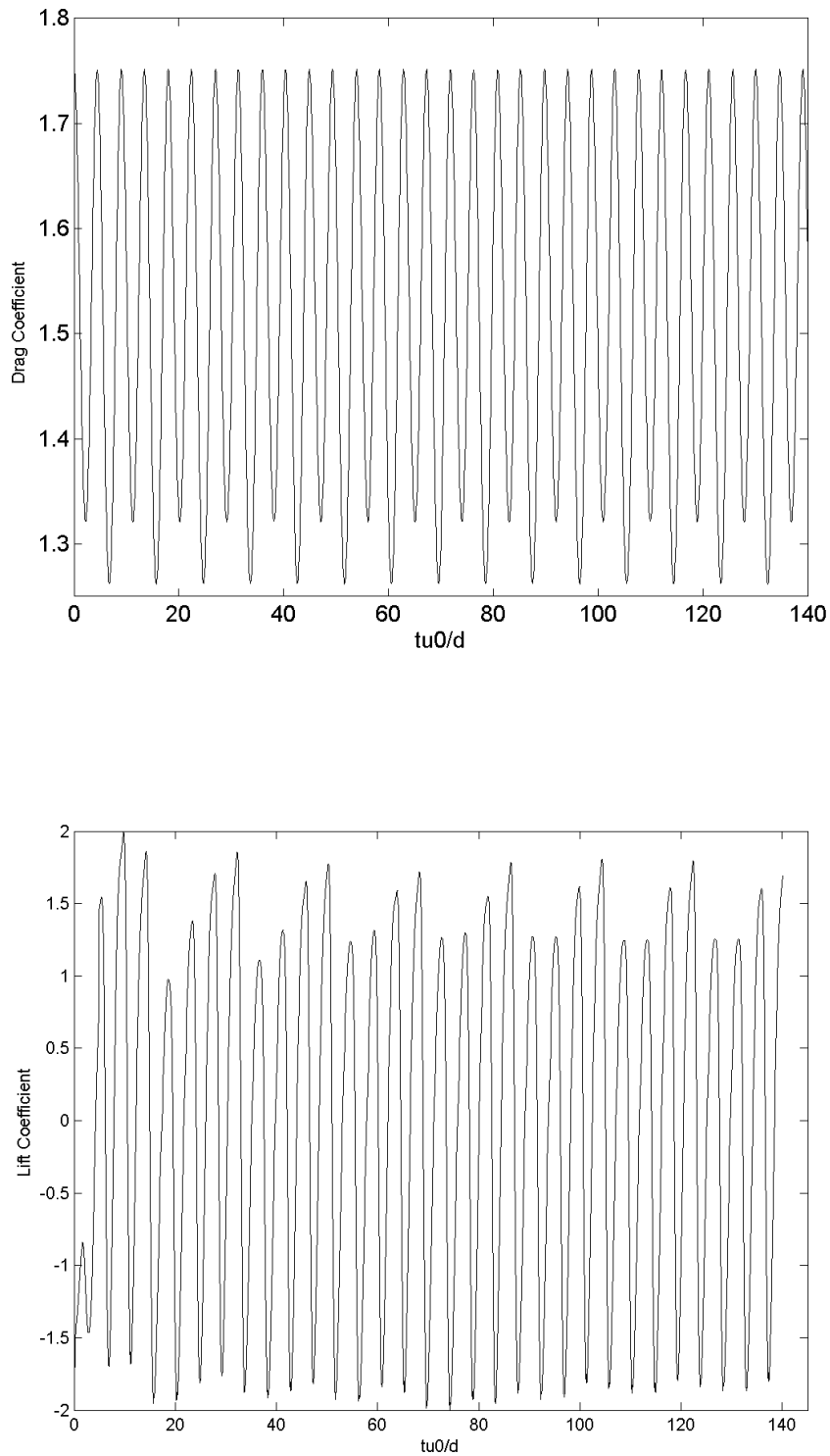


Figure 7. Aerodynamical Coefficients

5. CONCLUSIONS

Results of two-dimensional detached eddy simulation of the turbulent flow around a cylinder close to a plane were showed. Visualizations of instantaneous flow in the form of velocity vectors, streamlines, pressure and vorticity contours were presented. Instantaneous lift and drag coefficient results were showed, as well as the calculated Strouhal number and average drag.

The instantaneous flow visualizations showed the fast formation of low pressure zones at the cylinder surface. It is

noted that the vortices show a "mushroom" pattern. The lift coefficients present similar oscillatory behavior. This behavior is related to the vortex shedding. Therefore, it can be stated that the vortex shedding has an oscillatory pattern. The drag coefficient showed an oscillatory pattern, but one can note different amplitudes at certain moments.

One can conclude that the obtained results can be considered as consistent, because they are similar with numerical data for the same conditions at the literature. Experimentation must be conducted to validate the obtained data and to evaluate the physical mechanisms that are present on the flow. Besides, modifications at the DES formulation can be made to analyze the behavior of hybrid formulations on the turbulence.

6. REFERENCES

- Bearman, P. and Zdravkovich, M. "Flow around a circular cylinder near a plane boundary." *Journal of Fluid Mechanics*,89:33-47, 1978.
- Bimbato, A., Pereira L., and Hirata M. "Simulation of viscous flow around a circular cylinder near a moving ground." *Journal of the Brazilian Society of Mechanical Sciences and Engineering* 31:243-252, 2009.
- Chorin, A. J. "Numerical solution of the navier-stokes equations." *Mathematics of Computation* 22:745-762, 1968.
- Codina, R. . " Pressure stability in fractional step finite element methods for incompressible flows." *Journal of Computational Physics* 170:112-140, 2001.
- Donea, J and Huerta, A " *Finite Element Method for Flow Problems*". Wiley, 2003.
- Goldberg, D. and Ruas, V. "A numerical study of projection algorithms in the finite element simulation of three-dimensional viscous incompressible flow." *International Journal for Numerical Methods in Fluids* 30:233-256, 1999.
- Guermond, J., Mineev, P. and Shen, J. "An overview of projection methods for incompressible flows." *Computer Methods in Applied Mechanics and Engineering* 195:6011–6045, 2006.
- Lei, C., Cheng, L., and Kavanagh, K. " Numerical flow visualization of vortex shedding flow over a circular cylinder near a plane boundary", 1999.
- Lohner, R., Yang,C., Cebal, J., Camelli ,F., Soto, O., and Waltz, J. "Improving the speed and accuracy of projection-type incompressible flow solvers." *Computer Methods in Applied Mechanics and Engineering* 195:3087–3109, 2006.
- Menter, F.R., Kuntz, M. and Langtry, R. "Ten years of industrial experience with the sst turbulence model." *Turbulence, heat and Mass transfer* 4, 2003.
- Mineev, P. "A stabilized incremental projection scheme for the incompressible navier-stokes equations." *International Journal for Numerical Methods in Fluids* 36:441-464, 2001.
- Nishino, T., Roberts, G. and Zhang, X. "Unsteady rans and detached-eddy simulations of flow around a circular cylinder in ground effect." *Journal of Fluids and Structures* 24:18-33, 2008.
- Nishino, T. and Roberts, G.T. " Absolute and convective instabilities of two-dimensional bluff body wakes in ground effect". *European Journal of Mechanics B/Fluids* 27:539-551, 2008.
- Nishino, T., Roberts, G.T. and Zhang, X. " Vortex shedding from a circular cylinder near a moving ground." *Physics of Fluids* 19, 2007
- Silveira-Neto, A. " Fundamentos da turbulência nos fluidos." In A.P.S. Freire, P.Menut, and J.Su (Eds.), *Turbulência*, Volume 1, pp. 3-48. ABCM, 2001
- Strelets, M. "Detached eddy simulation of massively separated flows". *AIAA Journal* 2001- 0879, 2001.
- Zhang, X. (2007). " An adaptive phase field method for the mixture of two incompressible fluids." *Computers and Fluids* 36:1307-1318, 2007
- Zdravkovich, M. " Forces on a circular cylinder near a plane wall." *Applied Ocean Research* 7:197-201, 1985.
- Zienkiewicz, O.C., Taylor, R.L. and Nithiarasu, P. " *The Finite Element Method for Fluid Dynamics*" (6th ed.), 2005. Elsevier.

7. Responsibility notice

The author(s) is (are) the only responsible for the printed material included in this paper